Front. Earth Sci. 2023, 17(1): 18–29
https://doi.org/10.1007/s11707-022-1015-0

RESEARCH ARTICLE

Pore structure characteristics of low-rank coal reservoirs with different ash yields and their implications for recoverability of coalbed methane—a case study from the Erlian Basin, northeastern China

Dawei DONG[1], Jiaosheng YANG (✉)[2], Qiujia HU[3], Shitao CUI[4], Fenjin SUN[2], Jidong ZHANG[2], Xinrui CUI[3]

1 Shandong Institute of Petroleum and Chemical Technology, Dongying 257061, China
2 PetroChina Research institute of petroleum exploration and development, Beijing 100083, China
3 Shanxi CBM Exploration and Development Branch, PetroChina Huabei Oilfield Company, Changzhi 046000, China
4 China National Logging Corporation, Xi'an 710077, China

Abstract Pores are the main accumulation sites and migration pathways for coalbed methane (also referred to as CBM). Pore structure restricts the content and recoverability of CBM from coal reservoirs. In this study, 12 representative coal samples with different ash yields that have similar tectonic characteristics and burial depths were collected from different mining areas in the Jiergalangtu and Huolinhe depressions in the Erlian Basin. These samples were used to study the restrictions of ash yield on the characteristics of coal pore structures and the recoverability of CBM through macroscopic and microscopic structure observation, scanning electron microscope observations, vitrinite reflectance tests, low-temperature N_2 adsorption, nuclear magnetic resonance (NMR), and micro-computed tomography. The results show that coal reservoirs in the study area vary greatly in ash yield, based on which they can be divided into three types, i.e., low-ash-content, ash-bearing, and high-ash-content coal reservoirs. In addition, the ash yield has a certain impact on the development of coal pores; coal samples with lower ash yields indicate the presence of well-developed medium-large pores and better connectivity. Ash yield also has a certain impact on the brittleness of coal wherein a lower ash yield implies the development of brittle coal that is more liable to fracture as compared to less brittle samples at the same pressure. Absorbed gas content also varies significantly with ash yield; a low ash yield impacts the gas saturation of coal. Overall, for coal reservoirs in the study area, their porosity, pore diameter, movable fluid porosity, adsorbed gas amount, and recoverability decrease as the ash yield increases.

Keywords coal reservoir, ash, pore structure, recoverability, Erlian Basin

Received November 28, 2021; accepted April 15, 2022

E-mail: yangjs69@petrochina.com.cn

1 Introduction

Coal pores are spaces in the coal matrix that are not filled with solids; this makes them a type of complex porous media (Meyers, 1982; Fu et al., 2007; Liu et al., 2020a). Coalbed methane is usually stored in coal pores in an absorbed state. It is important to analyze the pore characteristics of coal which forms a vital basis for analyzing the reserves, flowability, and recoverability of CBM (Fu et al., 2017; Liu et al., 2017; Wang et al., 2017; Liu et al., 2018). The pore structure of coal affects pore size, reservoir connectivity, and the adsorption, diffusion, and penetration of CBM in coal reservoirs and can, to some extent, further influence its recoverability (Clarkson and Bustin, 1999; Yao and Liu, 2012; Wang et al., 2019). Structure properties, coal roof lithology and hydrogeology conditions have important influences on gas accumulation, preservation and enrichment (Meng et al., 2014). The reservoir pressure is a key factor of CBM productivity (Meng et al., 2020). The effect of coal metamorphism on the occurrence and enrichment of CBM has been the focus of several studies (Cai et al., 2016; Li et al., 2016, 2017; Zhao et al., 2016). The impact of coal deformation on the recoverability of CBM is also of importance since coal deformation influences coal

porosity and permeability (Zhu et al., 2016; Fu et al., 2017; Hou et al., 2017; Zhao et al., 2017a). As a common component of low-rank coal seams, ash has a considerable impact on the pore structure of coal seams. Ash in coal originates from residues resulting from the complete combustion of minerals in coal and is an important parameter for the assessment of coal quality (Zhou et al., 2011). A large volume of reports and studies exist on the pore structure of coal seams. Of these, a few focus on the impact of ash on pore structure and use analytical tools like low-temperature nitrogen adsorption, NMR, and argon ion polishing and imaging. The data suggests that in the case of low ash content, ash particles generally fill in pore throats and micropores, resulting in a decrease in fractal dimensions and an increase in heterogeneity (Zhang et al., 2019a; Wang, 2020; Jia et al., 2021). As compared with the samples which are not de-ashed, the de-ashed samples feature increased pore quantity, pore volume, pore-specific surface area, pore surface fractal dimensions, percentage of micropores, and total pore quantity; they also have a decreased mean pore diameter (Song et al., 2014). For example, the lignite and long flame coals with medium ash content and high content of volatiles in the Bayanhua sag in the Erlian Basin show considerable resource potential (Yao et al., 2020)

Yao et al. (2020) discovered that lignite and long flame coals with medium ash content and high volatile content have mainly developed in the Bayanhua sag in the Erlian Basin, showing considerable resource potential. Based on this, they further summarized the key geological elements and resource potential assessment methods of hugely-thick low-rank coal reservoirs. Previous studies merely incorporated a brief analysis of the ash yield as one of the factors. They lack a more comprehensive, systematic study on the impact of the ash yield on the porosity of pores and fissures.

Theoretical and experimental methods, including the fluid injection method, the spectrum testing method, and the image analysis method are applied in China and around the world to target the pore structure characteristics of coal (Li, 2018). Among them, the commonly used fluid injection method includes mercury injection, gas adsorption (N_2 and CO_2), and low-field NMR. In general, the CO_2 (or low-temperature N_2) adsorption method, combined with mercury injection, is mostly employed to quantitatively characterize the pores and fissures in coal reservoirs, to explore the distribution characteristics of pore specific surface area, pore volume, and pore diameter, and to study the fractal characteristics of pores and fissures of different sizes based on different mathematical models (Yao et al., 2008, 2009a; Jiang et al., 2011; Clarkson et al., 2013; Liu et al., 2020a; Yang et al., 2020). Yao et al. (2010), Yao and Liu (2012) first established the conversion relationship between T2 relaxation time and the porosity and pore-diameter distribution of coal reservoirs by analyzing NMR relaxation time. These results proved the feasibility and effectiveness of the application of NMR in characterizing pores and fissures of coal reservoirs (Zheng et al., 2018; Kang et al., 2019; Zhang et al., 2019b). Despite its wide application in characterizing pores and fissures of coal reservoirs, the fluid injection method can only be used to test open pores. The limitations of experimental methods do not allow the characterization of closed pores. In recent years, multiple non-destructive and highly-efficient non-fluid-injection testing techniques have been gradually applied to the quantitative characterization of pores and fissures in coal reservoirs, such as small-angle neutron scattering (SANS), small-angle X-ray scattering (SAXS), focused ion beam-scanning electron microscope (FIB-SEM), and micro-computed tomography (μ-CT). Owing to the low requirements on coal samples, the SAXS and SANS techniques are suitable for fragile samples that are tough to acquire through coring; these methods are also nondestructive to samples during testing (Sakurovs et al., 2012; Clarkson et al., 2013; Cai et al., 2014; Zhao et al., 2014; Okolo et al., 2015; Liu et al., 2020b). FIB-SEM and μ-CT technology allow continuous scanning and 3D reconstruction, which are conducive to the study of pores and fissures in coal reservoirs. They effectively reveal the 3D continuous changes of the pores and fissures, and can also reflect the characteristics of strong heterogeneity within the pores and fissures (Watanabe et al., 2011; Golab et al., 2013; Jing et al., 2016, 2017; Li et al., 2017; Liu et al., 2017; Zhou et al., 2017; Jiu et al., 2021; Wang and Mao, 2021). For the image analysis technique, the pores and fissures in coal reservoirs are observed under a microscope, followed by image acquisition and the analysis of the size, shape, connectivity, and surface morphology characteristics of pores and fissures. Image analysis techniques mainly include scanning electron microscopy (SEM), field emission scanning electron microscopy (FESEM), transmission electron microscopy (TEM), and atomic force microscopy (AFM) (Harris and Yust, 1976; Li et al., 2012; Liu et al., 2014, 2021; Nie et al., 2015; Zhao et al., 2017b; Huang and Liu, 2019). Individual methods differ in the scale of pore characterization due to different testing principles and media. Since pores in coal reservoirs cannot be completely characterized using a single method, it is necessary to combine the aforementioned testing methods to comprehensively characterize the pore–fissure system and to study the degree of coal metamorphism and pore characteristics.

The Erlian Basin is characterized by widely developed coal seams, ubiquitous gas logging anomalies, and rich resources of CBM, which make it a favorable region for low-rank CBM exploration in China. The Lower Cretaceous coal seams in the Huolinhe and Jiergalangtu depressions on the eastern end of the Erlian Basin are similar in burial depth, metamorphic grade, tectonics but differ greatly in pore structure and the recoverability of

CBM. In this study, representative coal samples were collected from the Jiergalangtu and Huolinhe Depressions in the Erlian Basin. They were used to study the impacts of the ash yield on the characteristics of coal pore structures and to analyze the restrictions of the recoverability on CBM through macroscopic and microscopic structure observations, observation under a scanning electron microscope, vitrinite reflectance tests, low-temperature N_2 adsorption, NMR, and micron-CT analysis of the samples. The purpose is to further clarify the impact of ash on the pore structure of coal and to provide references for research and production— related to CBM.

2 Geological setting

The Erlian Basin is a Mesozoic–Cenozoic coal-bearing rift valley that developed within the folded basement of the Hercynian geosyncline in the Tianshan–Xingmeng Fold Belt. It has undergone five periods of basic tectonic evolution, including the fault depression during the Early–Mid Jurassic, tectonic reversion during the Late Jurassic (accompanied with intense volcanism), massive fault depression in the early Early Cretaceous, tectonic the reversion in the late Early Cretaceous, and uplift since the Late Cretaceous, resulting in the formation of 47 coal-bearing depressions in total (Sun et al., 2017). In the Erlian Basin, the depressions are relatively independent of each other and have independent sedimentary systems while their sediments have multiple provenances and contain coarse debris, as a result of their proximity to source areas. Two coal-bearing formations, the Mid-Lower Jurassic Alatanheli Group and the Hantala Formation of the Lower–Cretaceous Bayanhua Group, developed in the periods of initial tension cracking and shrinkage during the tectonic evolution of the basin. Of these two formations, the latter is the main coal-bearing strata in the Erlian Basin (Sun et al., 2017). This paper focuses on the Huolinhe Depression in the northeastern part of the Erlian Basin and the Jiergalangtu Depression in the center (Fig. 1).

The Huolinhe Depression is a long and narrow coal-bearing basin that spreads in the NE strike. It is approximately 60 km long and 9 km wide on average, covering an area of 540 km^2. Its coal-bearing strata formed in the Lower Cretaceous, and the coal seam depth is generally less than 1000 m, with proven coal reserves of 1.31 × 10^{10} t. The Jiergalangtu sag, which is located in a suburb of Xilinhot City, is a dustpan-shaped NE-strike depression that is faulted in the north-west and overlapped in the south-east. It has a length of approximately 67 km, a width of 7–20 km, and an area of 1100 km^2. The coal-bearing strata in the Jiergalangtu Depression include Mid and Lower Jurassic coal seams with depth generally less than 1500 m, as well as Lower Cretaceous coal seams with depth generally less than 1000 m.

The coal seams in the Huolinhe Depression are generally made-up of less than 0.5% vitrinite; they are mainly composed of lignite. The coal seams in the Jiergalangtu Depression are mainly composed of lignite too, with generally 0.32%–0.47% vitrinite. Developed under the control of plutonic metamorphism, the metamorphic grade of coal in the Jiergalangtu Depression is mainly controlled by the depth of its coal seams. The deeper the coal seam, the bigger the R_o (Fig. 2). As the Cretaceous coal seams in the Huolinhe and Jiergalangtu Depressions are similar in depth, their metamorphic grades are somewhat similar.

3 Methods

3.1 Sample collection

To assess the characteristics of pore structures of coal reservoirs with different ash yields, 13 mines located in

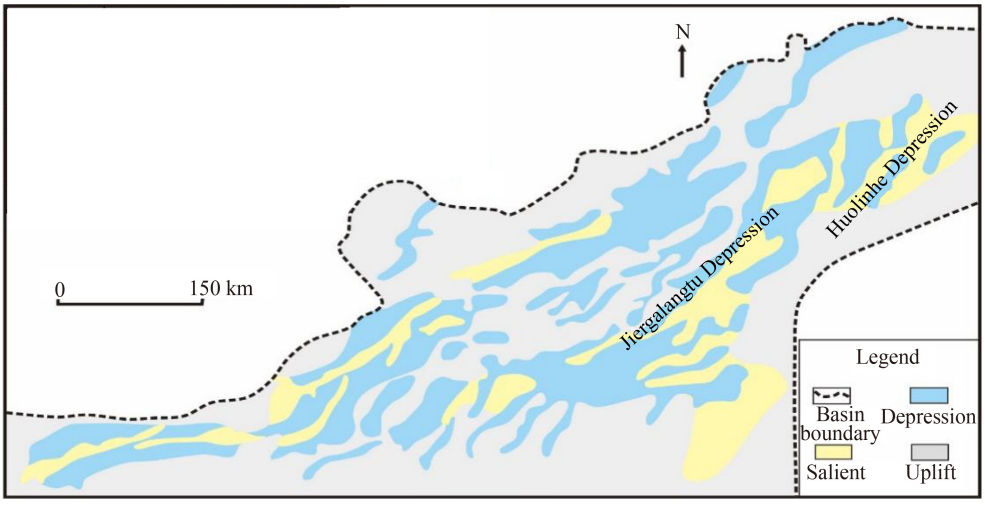

Fig. 1 Division of tectonic units and location of study area in the Erlian Basin (modified after Zhao et al., 2015).

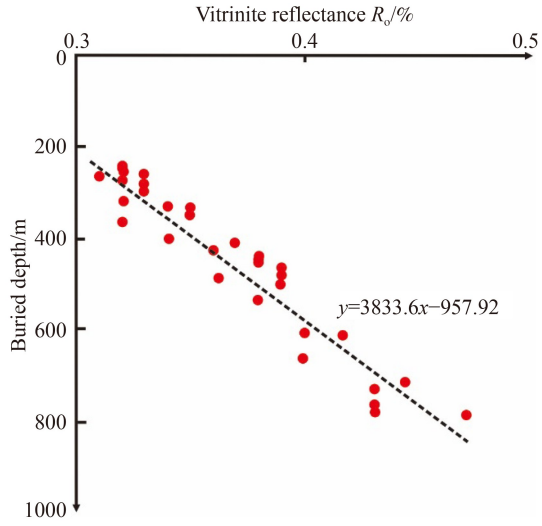

Fig. 2 Relationship between R_o and burial depth of coal in the Huolinhe and Jiergalangtu depressions, Erlian Basin.

the Lower Cretaceous of the Huolinhe and Jiergalangtu depressions were selected for underground observations and to collect samples. During sampling, the different impact levels of tectonism and magmation on samples were taken into consideration. Twelve representative coal samples that are similar in both structural features and depth were selected to be measured for their ash yield. The samples were subsequently analyzed with SEM, micron-CT, NMR, and low-temperature N_2 adsorption experiments. Data from the experimental analysis of the 12 samples are shown in Table 1.

3.2 Experimental tests

Analytical techniques like SEM, micron-CT scanning, NMR, and low-temperature N_2 adsorption are used to analyze the characteristics of micropore structures, fissure development, movable fluid pores, and adsorption–desorption of coal in the Erlian Basin. These experiments were conducted at laboratories of the PetroChina Institute for Exploration and Development in Langfang, China. SEM and micron-CT analysis were conducted using the environmental scanning microscope ESEM2020 and the micron-CT analyzer MICRO XCT-400, respectively to qualitatively determine how the pores in coal rocks formed.

The NMR testing experiment used a low-field NMR core analyzer RecCore-2500 to analyze the overall porosity of the coal samples. Nearly 9 cm^3 of fresh samples were taken from larger coal samples and placed in a vacuum oven and dried at 65°C until their weight was constant, after which they were placed in a saturated solution KCl for over 24 h. The samples were then centrifuged at high speed and at 200 Psi for 1.5 h, and then tested by NMR; each sample was tested twice. The T_2 relaxation spectrum under saturated water reflects the distribution of pore sizes throughout the sample. The differences between the T_2 relaxation spectrum under the state of saturated water and that under the state of bound water can reflect the quantity of the movable fluid pores in the sample in water.

For the low-temperature N_2 adsorption experiment, the low-temperature liquid nitrogen absorption Tristar 23020 was used. Samples were ground and sieved to 60–80 meshes. Two samples of 2 g each were dried in an oven at a constant temperature of 105°C. After 3 h, the samples were moved to a vacuum chamber and degassed for 24 h. During the experiment, saturated pressure conditions at a temperature of 77.35 K were maintained. High-purity liquid nitrogen was used as the adsorption medium to conduct the adsorption-desorption experiment under different relative pressures.

Table 1 Experimental samples and experiments

Sample No.	Burial depth/m	Ash yield/%	Experimental items			
			SEM	Micron CT	NMR	Low-temperature N_2 adsorption
JM1	421	32.12	√	√	√	
JM2	435	15.23	√	√	√	
JM3	455	35.41	√		√	
HM1	463	37.56	√		√	
HM2	475	41.47	√		√	
HM3	455	9.74	√	√	√	
JM4	451	12.55				√
JM5	443	13.35				√
JM6	426	30.98				√
JM7	431	40.32				√
JM8	448	34.12				√
HM4	459	22.66				√

4 Results

4.1 Analysis of pore types

Six samples with different ash yields were observed by SEM (Fig. 3). However, only the characteristics of medium and large pores are observable as a result of the limited resolution of the SEM. There are mainly two types of coal pores in the study area: residual issue pores with regular shapes and coal-rock plant tissue pores with irregular shapes. Cell-cavity tissue pores, tissue pores, and plant cell residual pores mainly develop in xylem reserved in fusinites and semi-fusinites. The elliptical cellular structures are mainly xylem. Their longitudinal sections are irregular under the microscope, with some deformation affecting a small quantity of cell cavities. Based on pore diameter, and in accordance with the Hodot pore-size classification standard, coal pores can be classified into two types. The first type is transition pores-micropores with a pore radius less than 100 nm, which occur in large quantities except at the surface and make up 26% of the total surface porosity on average. The second type is the medium-large pores with a pore radius greater than 100 nm, which occur in relatively smaller quantities but make up the majority (74% on average) of the surface porosity. The pores of this type have a pore diameter of 4 μm–800 nm generally and a certain degree of connectivity. Comparing the SEM images of JM3 and JM2 shows that JM2 with low ash yield has better-developed medium-large pores and better connectivity.

The grid patterns of pores and fissures in coal are clear in the three samples scanned with micron–CT (Fig. 4); fissures are mostly in the shape of grids or branches— the higher the ash yield, the more severely the fissures are filled with minerals. In Fig. 4, the micron-CT scan of JM2 samples, with 15.23% ash yield, shows a large volume of massive open fissures and a very small volume of filled fissures. Based on the developed pattern, the fissures are divided into three types. The first type is the nearly-horizontal bedding fissures, which extend along the surface of the bedding plane and are narrow and not filled (Fig. 4). The second type is structural fissures generated under the impact of local tectonic stress; they occur perpendicular to the bedding surface and extend like planar branches with somewhat varying widths— generally, main structural fissures are wider compared to the considerably narrow branch fissures which thin out gradually; these fissures are not filled (Fig. 4). Lithogenetic evolutionary fissures are the third type of fissures formed by coal in the process of thermal evolution; these form small planar grids, which in section show multiple small fissures forming some complex flower- or X-shaped patterns; in comparison with the two aforementioned types of fissures, lithogenetic evolutionary fissures are very small in volume, and appear blue in CT images (Fig. 4). Combining these results with those from the SEM experiment suggests that bedding and structural fissures have better connectivity and can form effective seepage passages favoring the seepage of CBM. The difference in development between the fissures in JM2 and JM3 is that JM2, with a low ash yield, has more developed fissures. This indicates that ash yield has some impact on the brittleness of coal; lower ash yields suggest relatively brittle coal which is more vulnerable to fissuring, compared to less brittle samples, at the same stress levels.

4.2 Nuclear magnetic resonance analysis

The relationship between relaxation time and pore diameter is obtained by performing mercury penetration and NMR experiments on samples. Pressure values of the Hg injection are first converted into pore diameter to plot the probability distribution frequency curve of Hg saturation versus pore diameter, which is used, together with the curve from the NMR experiment, to establish the relationship between pore diameter and relaxation time

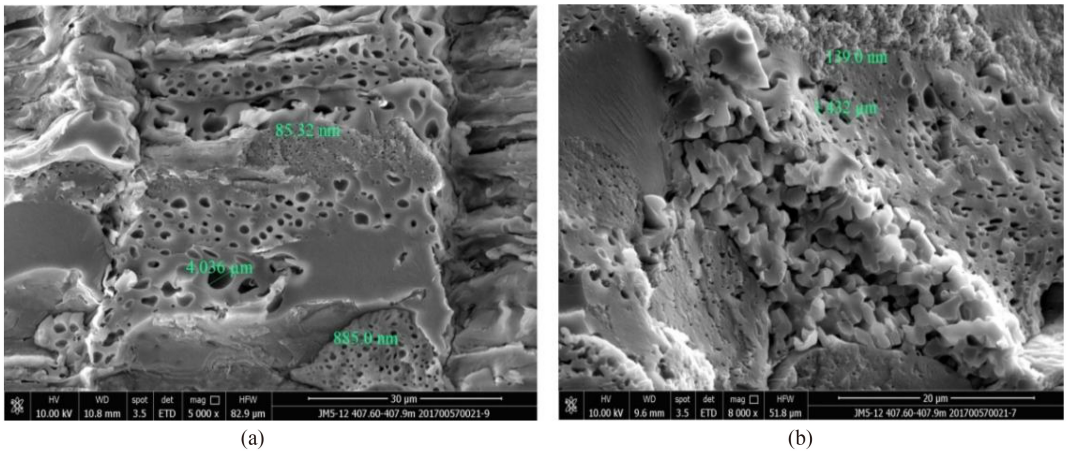

(a) (b)

Fig. 3 Typical scanning electron microscope images of JM3 and JM2. (a) Scanning electron microscope image of JM3; (b) scanning electron microscope image of JM2.

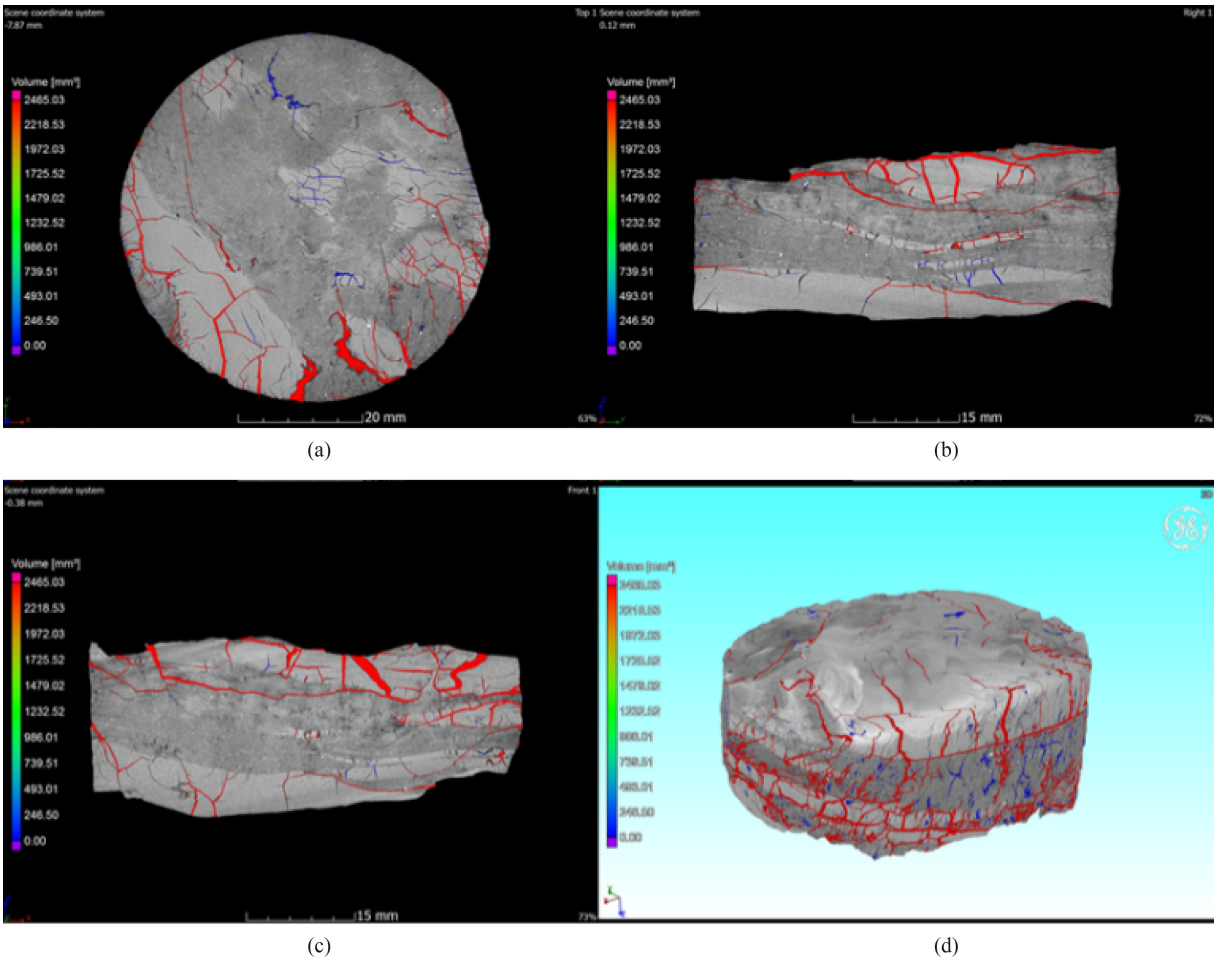

Fig. 4 CT Scanning of JM2 in the Jiergalangtu Depression. (a) Development characteristics of micro-fissures parallel to strata (section in the XY direction); (b) development characteristics of micro-fissures parallel to strata (section in the *XZ* direction); (c) development characteristics of micro-fissures parallel to strata (section in the *YZ* direction); (d) 3D view of rock skeleton and micro-fissures.

through the deformation and stretching of the horizontal and vertical coordinates (Fig. 5). That is, the transverse relaxation time corresponds to pore sizes 0.1 μm and 1 μm is 2.5 ms and 20 ms, respectively.

In combination with the results from this NMR test (Fig. 6(a)), coal pores are divided into three types by pore diameter—micro-small pores with diameter less than 0.1 μm, medium pores with diameter more than 0.1 μm but less than 1 μm, and large pores with diameter more than 1 μm and fissures.

Experimental results from the six samples suggest that the T_2 spectrum of coal pores is characterized by a single peak; larger peak areas correspond to better developed pores. For the spectrum peaks of these six samples, the T_2 relaxation time mainly ranges between 0.5 and 10 ms, the peak appears close to 3 ms, the signal intensity of the peaks develops between 600 and 1600, and the span is larger. This suggests that, in the study area, coal pores are uneven in diameter and there is considerable variation in their pore diameter. Micropores, small pores, medium pores, and fissures are well developed in the study area. The difference in the NMR and SEM experimental results stems mainly from the difference in their measurement precision. The NMR precision is higher and can better reflect the impact of micro-small pores.

The movable fluid pores are mainly medium in size, with a lower limit of 25 ms; the approximate pore diameter is 1 μm (Fig. 6(b)). Large pores and fissures have good movability but fissures have limited volume and do not constitute the main reservoir space. Micro-small pores are mainly adsorptive pores, occupied by bound water and poor in movability. By comparing samples JM1 and HM3, it is found that their lower limits of pore movability are similar, but the volume of movable fluid pores varies greatly. For samples JM1, the T_2 spectrum from NMR shows large porosity, and so the volume of corresponding movable fluid pores is large.

Experimental results show that the curves of samples with a high ash yield have low signal intensity and the peak value shifts toward the left (closer to the graphical origin) compared to the samples with low ash yield. This indicates an increase in the number of micro-small pores

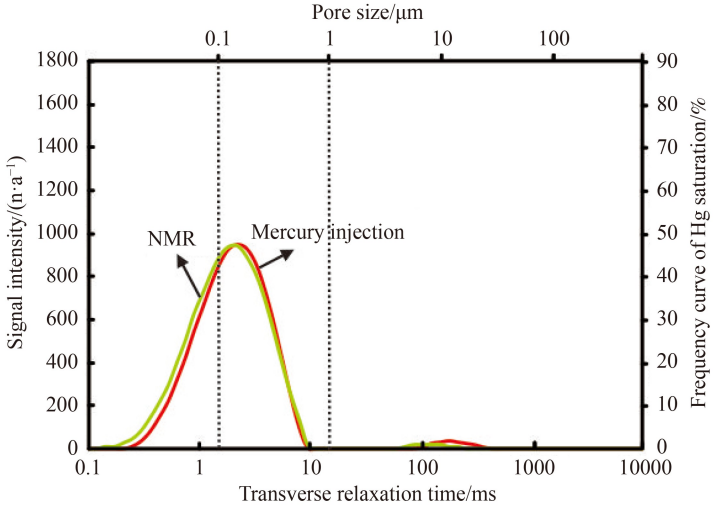

Fig. 5 Relation between relaxation time and aperture conversion.

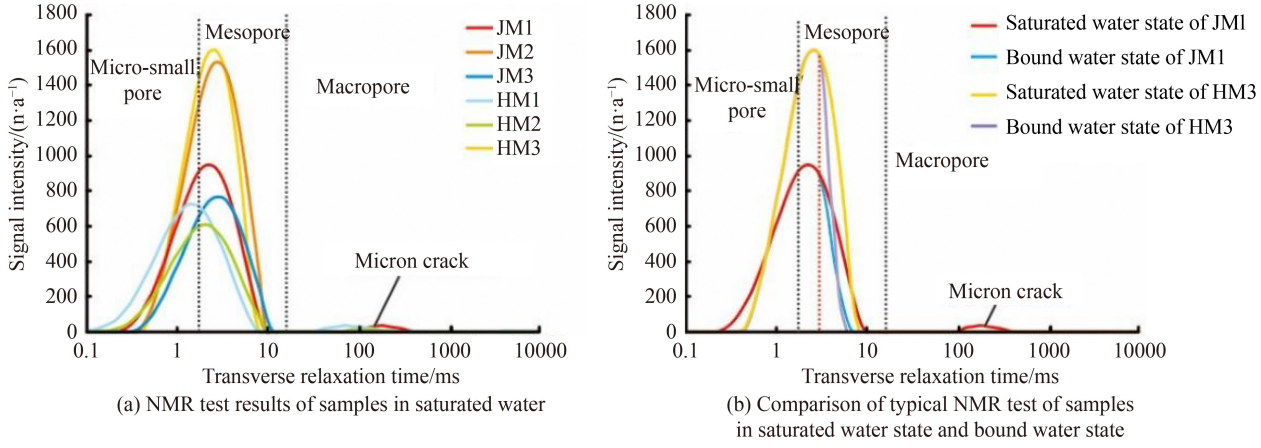

Fig. 6 NMR T2 distribution of coal samples from Huolinhe and Jiergalangtu Depressions, Erlian basin.

and reinforces that coal seams with high ash yield have more developed micro-small pores.

4.3 Analysis of N_2 adsorption curves

Low-temperature N_2 adsorption mainly reflects the distribution of micro-small pores; it is not effective (i.e., shows weak adsorption) for medium and large pores. The liquid nitrogen adsorption curves (Fig. 7) suggest that mainly two types of pores develop in coal reservoirs—semi-open pores and open gas pores. Open gas pores are characterized by an adsorption curve that is relatively independent of the desorption curve; however, once the relative pressure is more than 0.8, both curves rise steeply. This is the case for samples with lower ash yield, such as JM4, HM4, and HM5; such pores play a more crucial role in spreading, adsorbing, and desorbing CBM. Semi-open pores are mainly characterized by a desorption curve that generally coincides with the adsorption curve, at a relative pressure of 0–0.3. This indicates that at low-pressure conditions, such pores are in the semi-closed

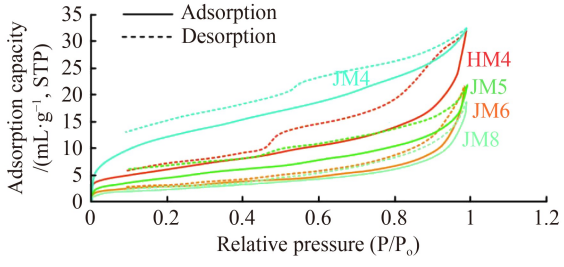

Fig. 7 Liquid nitrogen adsorption curves of coal samples from Houlinhe and Jiergalangtu Depressions,

condition; when the relative pressure is more than 0.3, the desorption curve separates from the adsorption curve, indicating the pores begin to open and morph into open gas pores—like the samples with higher ash yield, JM6, and JM8. Erlian Basin.

Converting the low-temperature N_2 adsorption curves into pore diameter distribution shows that when the micro-small pore distribution of samples JM6 and JM8 have high ash yields, micropores are more significant in

number; however, in the case of the micro-small pore distribution of samples JM4, JM5, and HM4 which have low ash yields, small pores dominate (Fig. 8).

5 Discussion

5.1 Classification of coal reservoir types

The water content and the content of volatile components in coal seams in the Erlian Basin do not change much; they range between 12.66%–20.22% and 41.16%–50.19%, respectively. The ash yield of coal has a more significant variation (9.74%–41.47%), based on which coal seams in the study area can be divided into three types: low-ash-bearing coal (Type I, ash yield < 10%), ash-bearing coal (Type II, ash yield: 10%–25%) and ash coal (Type III, ash yield: 25%–50%).

5.2 Analysis on pore structure of coal with different ash yields

Ash is the inorganic content of coal. Inorganics, when filled in coal pores and fissures, lower the porosity and permeability of coal. Its presence can impact the properties of coal reservoirs significantly (Liu et al., 2021). In the study area, the coal seams vary greatly in ash yield. This makes the ash yield a vital and basic parameter that affects the conditions of physical properties as well as the quality of coal reservoirs. It is important to investigate the impact of the ash yield on the quality of coal reservoirs.

Experimental results suggest the impact of ash yield on porosity can be estimated statistically (Fig. 9). Data from different experiments follow the same basic trend, which is that the ash yield results in decreased porosity—both porosity and fissure porosity reduce. This indicates that the ash yield not only has an impact on pores but also has an effect on fissures, with the impact on fissures smaller than that on pores (Fig. 9(a)). SEM and NMR experiments show that in the case of samples with ash yield less than 30%, porosity decreases quickly, whereas in the case of ash yield more than 30%, porosity changes (reduces) more slowly (Fig. 9(a)). The impact of the ash yield on pores of different sizes is also analyzed. It shows that ash yield strongly affects micro-small pores and, to a lesser extent, medium-large pores—both types of pores get smaller. However, it has a greater impact on medium-large pores; it reduces some medium-large pores to micro-small pores. This is also reflected in the gradual increase in the number of micro-small pores compared to medium-large pores as the ash yield increases (Fig. 9(b)).

Although the increased ash yield affects fissures, it has a greater effect on the movable fluid porosity (Fig. 10). μ-CT images show that, in the study area, structural fissures are vertical or near-vertical to the coal seam interface while bedding fissures run parallel or nearly parallel to the coal seam interface. The porosity of both types of fissures can be approximated using their 3D volumes picked up from CT scanning. As the ash yield increases, the porosity of both structural fissures and bedding fissures decreases. Ash yield has a larger effect on the latter primarily because ash deposition is also a product of sedimentation, and was likely contemporaneous with the deposits that evolved into coal seams. As a result, ash content increases significantly at the bedding surface (Fig. 10(a)). As the ash yield increases, the movable fluid porosity decreases. This is because the ash causes the medium-large pores which are the main flowable pores to be converted into micro-small pores which are predominantly non-flowable, adsorptive pores (Fig. 10(b)).

The N_2 adsorption experiment analyses the impact of ash yield on the volume of adsorbed and desorbed gas (Fig. 11). The results show that the ash yield has a greater impact on the adsorbed gas volume, especially in the case of low ash yield; this indicates that ash yield impacts the gas saturation of coal (Fig. 11(a)). Ash yield has a small

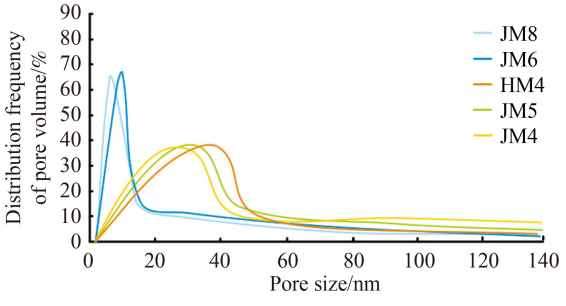

Fig. 8 Distribution characteristics of micro-pink pores in nitrogen adsorption at low temperature.

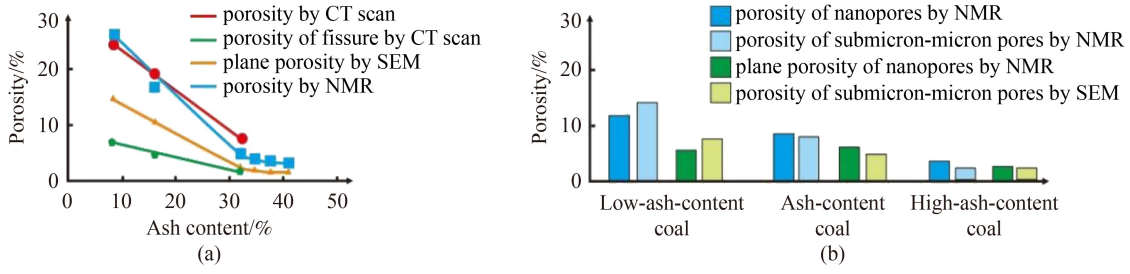

Fig. 9 Effect of ash content on porosity. (a) Effect of ash content on porosity; (b) effect of yield on pores of different sizes.

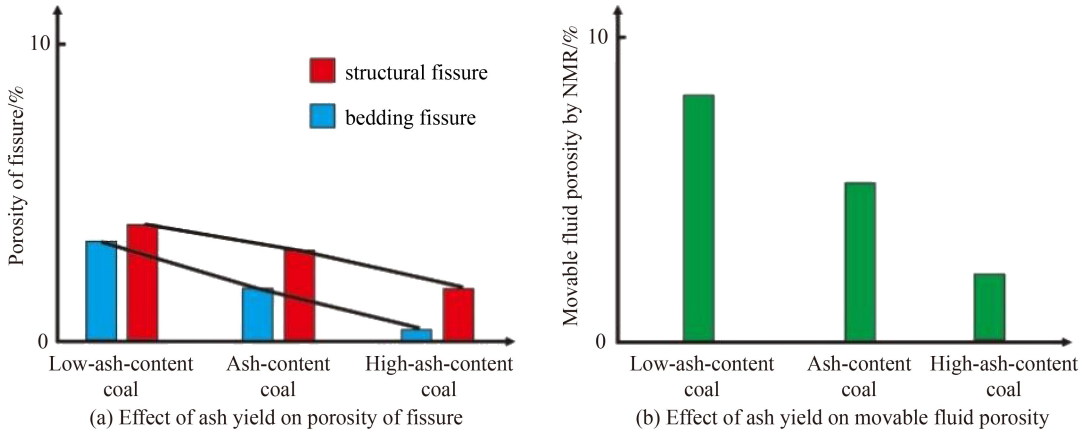

Fig. 10 Effects of ash content on fissures and movable porosity.

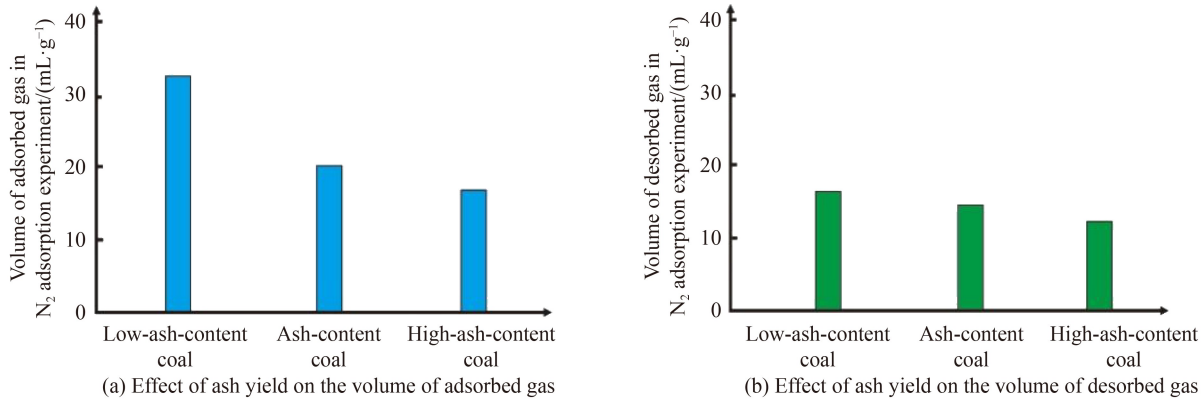

Fig. 11 Effect of ash content on adsorption amount and desorption amount.

impact on the desorbed gas volume. This is attributed to the impact of the conditions for the low-temperature N_2 adsorption experiment. The curves from the experiment (Fig. 7) show that as N_2 does not reach saturation in the experiment, it has a larger impact on the desorbed gas volume (Fig. 11(b)).

5.3 Impact of coal with different ash yields on recoverability of CBM

Factors like porosity, gas content, depth, and stratum pressure are typically considered in the evaluation of coal seams, while factors like the ash yield of coal and the recoverability of CBM are not as well studied. This study established the ash yield of coal as a critical, basic indicator of the quality of coal reservoirs which exerts an obvious controlling effect on porosity, pore structure, gas content, movable fluid porosity, and the volume of adsorbed and desorbed gas of CBM. Considering this, the ash yield of coal can be used as an indicator and can be combined with coal metamorphism to develop, in the future, a coal classification scheme that will play an important role in controlling the development of CBM.

As suggested by the presence of many well-developed medium-large pores, high porosity, well-developed bedding and structural fissures, high permeability and movable fluid porosity, and a large volume of adsorbed, desorbed, and recoverable gas, the analytical results from this paper show that low-ash-bearing coal is a kind-of-reservoir with the best recoverability. In comparison, ash-bearing coal has moderately-well-developed medium-large pores, porosity, bedding and structural fissures, permeability, moderate movable fluid porosity, and a moderate volume of adsorbed, desorbed, and recoverable gas. These characteristics make ash-bearing coal a kind-of-reservoir with good recoverability but less efficient than low-ash-bearing coal. Ash coal has fewer medium-large pores, low porosity, mainly micro-small pores, poorly-developed bedding and structural fissures which are mostly filled, low permeability, less movable fluid porosity, and lower volumes of adsorbed, desorbed, and recoverable gas. Therefore, ash coal is a kind-of-reservoir with poor recoverability.

6 Conclusions

1) For coal pores in the Erlian Basin, the micro-small pores significantly outnumber the medium-large pores. However, the latter accounts for much of the surface

porosity and have good connectivity. In the Erlian Basin, the movable fluid pores are mainly medium-large pores with a lower pore-size limit of 25 ms and an approximate pore diameter of 1 μm. Large pores and fissures have good movability, but fissures have limited volume and do not constitute the main reservoir space.

2) In the Erlian Basin, the ash yield of the coal shows a significant variation (9.74%–41.47%), based on which coal seams in the study area are divided into three types: Type I is low-ash-bearing coal with ash yield < 10%, Type II is ash-bearing coal with ash yield between 10%–25%, and Type III is ash coal with ash yield between 25%–50%.

3) Ash is the inorganic content in coal which, when filled in coal pores and fissures, lowers its porosity and permeability; its presence can impact the properties of coal reservoirs significantly. Thus, as a kind-of-reservoir low-ash-bearing coal in the Erlian Basin has the best recoverability for CBM. The recoverability of ash-bearing coal is not as efficient as the former, but is moderately better than that of ash coal, which has poor recoverability.

Acknowledgments This study was financially supported by the National Natural Science Foundation of China (Grant No. 42072162), the Natural Science Foundation of Shandong Province (No. ZR2020MD036), and a forward-looking and basic technology research project of PetroChina (No. 2021DJ2301).

References

Cai Y D, Liu D M, Pan Z J, Che Y, Liu Z H (2016). Investigating the effects of seepage-pores and fractures on coal permeability by fractal analysis. Transp Porous Media, 111(2): 479–497

Cai Y D, Liu D M, Pan Z J, Yao Y B, Li J Q, Qiu Y K (2014). Pore structure of selected Chinese coals with heating and pressurization treatments. Sci China Earth Sci, 57(7): 1567–1582

Clarkson C R, Bustin R M (1999). The effect of pore structure and gas pressure upon the transport properties of coal: a laboratory and modeling study. 2. Adsorption rate modeling. Fuel, 78(11): 1345–1362

Clarkson C R, Solano N, Bustin R M, Bustin A M M, Chalmers G R L, He L, Melnichenko Y B, Radlinski A P, Blach T P (2013). Pore structure characterization of North American shale gas reservoirs using USANS/SANS, gas adsorption, and mercury intrusion. Fuel, 103: 606–616

Fu H J, Tang D Z, Xu T, Xu H, Tao S, Li S, Yin Z Y, Chen B L, Zhang C, Wang L L (2017). Characteristics of pore structure and fractural dimension of low-rank coal: a case study of Lower Jurassic Xishayao coal in the southern Junggar Basin, NW China. Fuel, 193: 254–264

Fu X H, Qin Y, Wei C T (2007). Coalbed Methane Geology. Xuzhou: China University of Mining and Technology Press (in Chinese)

Golab A, Ward C R, Permana A, Lennox P, Botha P (2013). High-resolution three-dimensional imaging of coal using microfocus X-ray computed tomography, with special reference to modes of mineral occurrence. Int J Coal Geol, 113: 97–108

Harris L A, Yust C S (1976). Transmisssion electron microscope observations of porosity in coal. Fuel, 55(3): 233–236

Hou S H, Wang X M, Wang X J, Yuan Y D, Pan S, Wang X (2017). Pore structure characterization of low volatile bituminous coals with different particle size and tectonic deformation using low pressure gas adsorption. Int J Coal Geol, 183: 1–13

Huang T, Liu Z (2019). Analysis on pore structure characteristics and influencing factors of coal reservoir in Yushe-Wuxiang Block. Coal Sci Technol, 47(7): 227–233

Jia T F, Wang M, Gao X Y, Zhao J G, Zhu J Q (2021). Pore structure characteristics of low-rank coal reservoirs and evaluation of fractal models. Nat Gas Geosci, 32(3): 423–436

Jiang W P, Song X Z, Zhong L W (2011). Research on the pore properties of different coal body structure coals and the effects on gas outburst based on the low-temperature nitrogen adsorption method. J China Coal Soc, 36(4): 609–614 (in Chinese)

Jing Y, Armstrong R T, Mostaghimi P (2017). Digital coal: generation of fractured cores with microscale features. Fuel, 207: 93–101

Jing Y, Armstrong R T, Ramandi H L, Mostaghimi P (2016). Coal cleat reconstruction using micro-computed tomography imaging. Fuel, 181: 286–299

Jiu B, Huang W H, Shi J, Hao R L (2021). A method to extract the content, radius and specific surface area of maceral compositions in coal reservoirs based on image modeling. J Petrol Sci Eng, 201: 108419

Kang J Q, Fu X H, Li X, Liang S (2019). Nitrogen injection to enhance methane and water production: an experimental study using the LF-NMR relaxation method. Int J Coal Geol, 211: 103228

Li S, Tang D Z, Xu H, Yang Z (2012). The pore-fracture system properties of coalbed methane reservoirs in the Panguan Syncline, Guizhou, China. Geosci Front, 3(6): 853–862

Li Z T (2018). Evolution of Pore-fractures of Coal Reservoir and Its Impact on CBM Microcosmic Flow. Dissertation for Doctor Degree. Beijing: China University of Geosciences (Beijing) (in Chinese)

Li Z T, Liu D M, Cai Y D, Ranjith P G, Yao Y B (2017). Multi-scale quantitative characterization of 3-D pore-fracture networks in bituminous and anthracite coals using FIB-SEM tomography and X-ray μ-CT. Fuel, 209: 43–53

Li Z T, Liu D M, Cai Y D, Shi T L (2016). Investigation of methane diffusion in low-rank coals by a multiparous diffusion model. J Nat Gas Sci Eng, 33: 97–107

Liu D M, Liu Z H, Cai Y D (2020a). Research progress on accumulation mechanism and formation geological conditions of coalbed methane. Coal Sci Technol, 48(10): 1–16

Liu D M, Wang Y J, Cai Y D (2018). Analysis of main geological controls on coalbed methane enrichment and accumulation patterns in low rank coals. Coal Sci Technol, 46(6): 1–8

Liu H H, Farid I I, Sang S X, Shang J H, Wu H Y, Xu H J, Zhang P S, Liu Q M (2020b). Synthetical study on the difference and reason for the pore structure of the No.3 coal reservoir from the southern Qinshui Basin, China, using mercury intrusion porosimetry, low-temperature N_2 adsorption, low field nuclear magnetic resonance, and nuclear magnetic resonance cryoporometry. Energy Rep, 6: 1876–1887

Liu H H, Sang S X, Wang G G, Li M, Xu H, Liu S, Li J, Ren B, Zhao Z, Xie Y (2014). Block scale investigation on gas content of coalbed methane reservoirs in southern Qinshui Basin with statistical model and visual map. J Petrol Sci Eng, 114: 1–14

Liu J H, Wang S W, Su D M (2021). Study on pore development characteristics of low rank coal reservoirs in Erlian Basin group. Safety Coal Mines, 52(2): 7–12 (in Chinese)

Liu S Q, Sang S X, Wang G, Ma J S, Wang X, Wang W F, Du Y, Wang T (2017). FIB-SEM and X-ray CT characterization of interconnected pores in high-rank coal formed from regional metamorphism. J Nat Gas Sci Eng, 148: 21–31

Meng Y J, Tang D Z, Xu H, Gan Q, Yan T T (2020). Identifying the key factor of medium-rank coalbed methane productivity with gray relational analysis: a case study in Liulin area, Ordos Basin, China. Energy Sources A Recovery Util Environ Effects: 1–14

Meng Y J, Tang D Z, Xu H, Li C, Li L, Meng S Z (2014). Geological controls and coalbed methane production potential evaluation: a case study in Liulin area, eastern Ordos Basin, China. J Nat Gas Sci Eng, 21: 95–111

Meyers R A (1982). Coal Structure. New York: Academic Press

Nie B S, Liu X F, Yang L, Meng J, Li X (2015). Pore structure characterization of different rank coals using gas adsorption and scanning electron microscopy. Fuel, 158: 908–917

Okolo G N, Everson R C, Neomagus H W J P, Roberts M J, Sakurovs R (2015). Comparing the porosity and surface areas of coal as measured by gas adsorption, mercury intrusion and SAXS techniques. Fuel, 141: 293–304

Sakurovs R, He L L, Melnichenko Y B, Radlinski A P, Blach T, Lemmel H, Mildner D F R (2012). Pore size distribution and accessible pore size distribution in bituminous coals. Int J Coal Geol, 100: 51–64

Song X X, Tang L W, Li W, Zeng F G, Xiang J H (2014). Pore structure in tectonically deformed coals by small angle X-ray scattering. J China Coal Soc, 39(4): 719–724 (in Chinese)

Sun F J, Li W Z, Sun Q P, Sun B, Tian W G, Chen Y J, Chen Z H (2017). Low-rank coalbed methane exploration in Jiergalangtu Sag, Erlian basin. Acta Petrol Sin, 38(2): 485–492

Wang A M, Wei Y C, Yuan Y, Li C F, Li Y, Cao D Y (2017). Coalbed methane reservoir's pore-structure characterization of different macrolithotypes in the southern Junggar Basin of northwest China. Mar Pet Geol, 86: 675–688

Wang T, Deng Z, Hu H Y, Cao M L, Zhang B X, Jiao P F, Yu Z (2019). Study on characteristics comparison of low rank coal coalbed methane reservoirs at home and abroad. Coal Sci Technol, 47(9): 41–50 (in Chinese)

Wang Y Z(2020). Fractal characteristics of coal rock pores in the Baliancheng Mining Area, Hunchun Basin. J Southwest Petrol U (Sci & Tech Edi), 42(1): 57–68 (in Chinese)

Wang Y, Mao C (2021). Nano/micro pore structure and fractal characteristics of Baliancheng Coalfield in Hunchun Basin. J Nanosci Nanotechnol, 21(1): 682–692

Watanabe N, Ishibashi T, Hirano N, Tsuchiya N, Ohsaki Y, Tamagawa T, Tsuchiya Y, Okabe H (2011). Precise 3D numerical modeling of fracture flow coupled with X-ray computed tomography for reservoir core samples. SPE J, 16(3): 683–691

Yang F, He D, Ma D M, Duan Z H, Tian T, Fu D L (2020). Multi-scale joint characterization of micro-pore structure of low-rank coal reservoir. Lithologic Reservoirs, 32(3): 14–23 (in Chinese)

Yao H P, Lv W B, Wang K F, Li L, Li W H, Lin H T, Li F C, Li Z (2020). Key geological factors and evaluation methods for huge low-rank coalbed methane reservoirs: taking Bayanhua depression in Erlian basin as an example. Coal Geo Explor, 48(1): 85–95 (in Chinese)

Yao Y B, Liu D M (2012). Comparison of low-field NMR and mercury intrusion porosimetry in characterizing pore size distributions of coals. Fuel, 95: 152–158

Yao Y B, Liu D M, Che Y, Tang D Z, Tang S H, Huang W H (2010). Petrophysical characterization of coals by low-field nuclear magnetic resonance (NMR). Fuel, 89(7): 1371–1380

Yao Y B, Liu D M, Tang D Z, Tang S H, Huang W H (2008). Fractal characterization of adsorption-pores of coals from north China: an investigation on CH_4 adsorption capacity of coals. Int J Coal Geol, 73(1): 27–42

Yao Y B, Liu D M, Tang D Z, Tang S H, Huang W H, Liu Z H, Che Y (2009). Fractal characterization of seepage-pores of coals from China: an investigation on permeability of coals. Comput Geosci, 35(6): 1159–1166

Zhang J J, Wei C T, Ju W, Yan G Y, Lu G W, Hou X W, Kai Z (2019a). Stress sensitivity characterization and heterogeneous variation of the pore-fracture system in middle-high rank coals reservoir based on NMR experiments. Fuel, 238: 331–344

Zhang J J, Wei C, Vandeginste V, Ju W, Qin Z, Quan F, Soh Tamehe L (2019b). Experimental simulation study on water migration and methane depressurizing desorption based on nuclear magnetic resonance technology: a case study of middle-rank coals from the Panguan syncline in the western Guizhou region. Energy Fuels, 33(9): 7993–8006

Zhao D F, Guo Y H, Mao X X, Lu C G, Li M, Qian F C (2017a). Characteristics of macro-nanopores in anthracite coal based on mercury injection, nitrogen adsorption and FE-SEM. J China Coal Soc, 42(6): 1517–1526 (in Chinese)

Zhao J L, Xu H, Tang D Z, Mathews J P, Li S, Tao S (2016). A comparative evaluation of coal specific surface area by CO_2 and N_2 adsorption and its influence on CH_4 adsorption capacity at different pore sizes. Fuel, 183: 420–431

Zhao X Z, Liu G D, Jin F M, Huang Z L, Lu X J, Sun M L, Ding X J,

Chen Z L (2015). Distribution features and pattern of effective source rock in small faulted lacustrine basin: a case study of the Lower Cretaceous in Erlian Basin. Acta Petrol Sin, 36(6): 641–652

Zhao Y X, Liu S M, Elsworth D, Jiang Y D, Zhu J (2014). Pore structure characterization of coal by synchrotron small-angle X ray scattering and transmission electron microscopy. Energy Fuels, 28(6): 3704–3711

Zhao Y X, Sun Y F, Liu S M, Wang K, Jiang Y D (2017b). Pore structure characterization of coal by NMR cryoporometry. Fuel, 190: 359–369

Zheng S J, Yao Y B, Liu D M, Cai Y D, Liu Y (2018). Characterizations of full-scale pore size distribution, porosity and permeability of coals: a novel methodology by nuclear magnetic resonance and fractal analysis theory. Int J Coal Geol, 196: 148–158

Zhou S D, Liu D M, Cai Y D, Yao Y B, Li Z T (2017). 3D characterization and quantitative evaluation of pore-fracture networks of two Chinese coals using FIB-SEM tomography. Int J Coal Geol, 174: 41–54

Zhou Y L, Liu N, Liu Q R (2011). Plant Biology. Beijing: Higher Education Press (in Chinese)

Zhu J F, Liu J Z, Yang Y M, Cheng J, Zhou J H, Cen K F (2016). Fractal characteristics of pore structures in 13 coal specimens: relationship among fractal dimension, pore structure parameter, and slurry ability of coal. Fuel Process Technol, 149: 256–267